

AD-A053 783 AIR FORCE MATERIALS LAB WRIGHT-PATTERSON AFB OHIO  
NOTCHED-FATIGUE BEHAVIOR TO 7075-BASE ALUMINUM ALLOYS. (U)  
FEB 78 J S SANTNER, J F SANTNER

F/G 11/6

UNCLASSIFIED

AFML-TR-77-78

NL

| OF |  
AD  
A053 783



END  
DATE  
FILED  
6-78  
DDC

AU NO. \_\_\_\_\_  
DDC FILE COPY

AD A 053783

AFML-TR-77-78

12  
B.S.

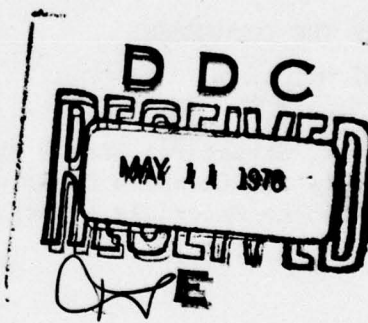
## NOTCHED-FATIGUE BEHAVIOR OF 7075-BASE ALUMINUM ALLOYS

JOSEPH S. SANTNER  
STRUCTURAL MATERIALS BRANCH  
METALS AND CERAMICS DIVISION

JOSEPH F. SANTNER  
NATIONAL TRAINING AND OPERATIONAL TECHNOLOGY CENTER  
U. S. ENVIRONMENTAL PROTECTION AGENCY

FEBRUARY 1978

TECHNICAL REPORT AFML-TR-77-78  
Final Report for Period January 1976 – August 1976



Approved for public release; distribution unlimited.

AIR FORCE MATERIALS LABORATORY  
AIR FORCE WRIGHT AERONAUTICAL LABORATORIES  
AIR FORCE SYSTEMS COMMAND  
WRIGHT-PATTERSON AIR FORCE BASE, OHIO 45433

NOTICE

When Government drawings, specifications, or other data are used for any purpose other than in connection with a definitely related Government procurement operation, the United States Government thereby incurs no responsibility nor any obligation whatsoever; and the fact that the government may have formulated, furnished, or in any way supplied the said drawings, specifications, or other data, is not to be regarded by implication or otherwise as in any manner licensing the holder or any other person or corporation, or conveying any rights or permission to manufacture, use, or sell any patented invention that may in any way be related thereto.

This report has been reviewed by the Information Office (IO) and is releasable to the National Technical Information Service (NTIS). At NTIS, it will be available to the general public, including foreign nations.

This technical report has been reviewed and is approved for publication.

*L.R.Bidwell*

L. R. Bidwell  
Program Manager

*621021*

FOR THE COMMANDER

*N. Tupper*  
N. TUPPER  
Chief, Structural Metals Branch  
Metals and Ceramics Division  
Air Force Materials Laboratory

Copies of this report should not be returned unless return is required by security considerations, contractual obligations, or notice on a specific document.

## UNCLASSIFIED

SECURITY CLASSIFICATION OF THIS PAGE (When Data Entered)

REPORT DOCUMENTATION PAGE		READ INSTRUCTIONS BEFORE COMPLETING FORM
1. REPORT NUMBER <b>(14) AFML-TR-77-78</b>	2. GOVT ACCESSION NO.	3. RECIPIENT'S CATALOG NUMBER <b>(9)</b>
4. TITLE (and Subtitle) <b>(6) NOTCHED-FATIGUE BEHAVIOR OF 7075-BASE ALUMINUM ALLOYS,</b>	5. TYPE OF REPORT & PERIOD COVERED Final report, covering period <b>January 1976-August 1976</b>	
7. AUTHOR(s) <b>(10) JOSEPH S. SANTNER</b> <b>JOSEPH F. SANTNER</b>	6. PERFORMING ORG. REPORT NUMBER <b>(11) 73510580 995</b>	
8. CONTRACT OR GRANT NUMBER(s)	10. PROGRAM ELEMENT, PROJECT, TASK AREA & WORK UNIT NUMBERS	
9. PERFORMING ORGANIZATION NAME AND ADDRESS Air Force Materials Laboratory (LLS) Air Force Wright Aeronautical Laboratories Wright-Patterson AFB, OH 45433	11. CONTROLLING OFFICE NAME AND ADDRESS Air Force Materials Laboratory (LLS) Air Force Wright Aeronautical Laboratories Wright-Patterson AFB, OH 45433	
12. MONITORING AGENCY NAME & ADDRESS (if different from Controlling Office) <b>(12) 55P.</b>	13. REPORT DATE <b>(11) February 1978</b>	
14. DISTRIBUTION STATEMENT (of this Report)  Approved for public release; distribution unlimited.	15. SECURITY CLASS. (of this report) <b>Unclassified</b>	
16. DISTRIBUTION STATEMENT (of the abstract entered in Block 20, if different from Report)	15a. DECLASSIFICATION/DOWNGRADING SCHEDULE	
17. SUPPLEMENTARY NOTES		
18. KEY WORDS (Continue on reverse side if necessary and identify by block number) Notched Fatigue      Analysis of Variance 7075-Base Alloys      Corrosion-Fatigue Purity Level Dispersoid Type	19. ABSTRACT (Continue on reverse side if necessary and identify by block number) Ten different alloys based on the 7075 composition were utilized to study the effects of purity level (w/o Fe+Si) and dispersoid type on the notched fatigue behavior in two different environments. These same alloys were used in other AFML investigations to determine how the various precipitates found in commercial 7000 series aluminum alloys control the mechanical properties. Purity significantly affects the notched ( $K_t=3$ ) fatigue life only in an inert test environment at the lowest load tested. Purity did not significantly affect (Over) → over	

**012329****JB**

**UNCLASSIFIED**

SECURITY CLASSIFICATION OF THIS PAGE(When Data Entered)

**20. Abstract**

the notched fatigue life when tests were conducted in an aggressive test environment. While the dispersoid type did change the macroscopic fracture appearance of the test specimen, this produced a small change in the notched fatigue life which was not significant at the one percent alpha level.

By far, the test environment was more important than the metallurgical variables considered. This is somewhat surprising since the duration of the tests were at most two days, allowing little time for corrosion. It appears that specifying stricter alloy purity levels or different dispersoid types will not improve the notched fatigue life of wrought 7000 series aluminum alloys.

ACCESSION for	
NTIS	White Section <input checked="" type="checkbox"/>
DDC	Buff Section <input type="checkbox"/>
UNANNOUNCED	<input type="checkbox"/>
JUSTIFICATION.....	
BY.....	
DISTRIBUTION/AVAILABILITY CODES	
Dist.	AVAIL. and/or SPECIAL
A	

**UNCLASSIFIED**

SECURITY CLASSIFICATION OF THIS PAGE(When Data Entered)

## FOREWORD

The work described in this report was performed by the Structural Metals Branch, Metals and Ceramics Division, Air Force Materials Laboratory, Air Force Wright Aeronautical Laboratories, Air Force Systems Command, Wright-Patterson Air Force Base, OH. The Project Number was 7351, "Metallic Materials", and the Task Number was 735105, "High Strength Metallic Materials". The research was conducted between January 1976 and August 1976.

The mechanical testing was conducted by Mr. Ronald Elder, Systems Research Laboratories, (SRL), and Mr. Charles Smith, University of Cincinnati. Fractography was performed with the assistance of Mr. Allen Jackson (SRL). EDAX work was done by Mr. Brewster Strope, SRL. The computer runs for the analysis of variance were performed by Mr. Michael Dennis on the CDC 6400 computer. The manuscript was typed by Mrs. Sally Gardner, University of Cincinnati. The authors wish to thank Drs. Lawrence R. Bidwell and W.H. Reimann for reviewing the original manuscript and acknowledge the helpful critiques made by Messrs. Nathan Tupper and Allan Gunderson.

TABLE OF CONTENTS

SECTION	PAGE
I      INTRODUCTION . . . . .	1
II     EXPERIMENTAL PROCEDURE . . . . .	3
A. Material . . . . .	3
B. Testing . . . . .	3
III    RESULTS. . . . .	8
A. Data Analysis . . . . .	8
B. Effect of Alloy Composition . . . . .	15
C. Effect of Chemical Environment. . . . .	18
D. Ancillary Fractograph Studies . . . . .	23
IV    DISCUSSION . . . . .	28
V    CONCLUSIONS. . . . .	33
REFERENCES . . . . .	34
APPENDIX A: ANALYSIS OF VARIANCE ON NOTCHED FATIGUE DATA. . . . .	36

PREVIOUS PAGE NOT FILMED  
BLANK

LIST OF TABLES

TABLE	PAGE
1. Comparison of Experimental and Commercial Alloys. . . . .	4
2. Notched Fatigue Life (Kilocycles) and Weibull Parameters of Experimental Aluminum Alloys Cycled at $\pm 12$ ksi (82.8 MPa) in an Oil Environment ( $R=-1$ , $K_t=3$ ) . . . . .	11
3. Notched Fatigue Life (Kilocycles) and Weibull Parameters of Experimental Aluminum Alloys Cycled at $\pm 18$ ksi (124.2 MPa) in an Oil Environment ( $R=-1$ , $K_t=3$ ) . . . . .	12
4. Notched Fatigue Life (Kilocycles) and Weibull Parameters of Experimental Aluminum Alloys Cycled at $\pm 12$ ksi (82.8 MPa) in a $3\frac{1}{2}\%$ Salt Water Environment ( $R=-1$ , $K_t=3$ ) . . . . .	13
5. Notched Fatigue Life (Kilocycles) and Weibull Parameters of Experimental Aluminum Alloys Cycled at $\pm 18$ ksi (124.2 MPa) in a $3\frac{1}{2}\%$ Salt Water Environment ( $R=-1$ , $K_t=3$ ). . . . .	14
6. Frequency Table Used to Determine if There is a Correlation Between the Dispersoid Type and the Macroscopic Fracture Appearance. . . . .	19
A1. The Nonequal Range for $N_f$ Between the Two Chemical Environments Among Four Experimental Alloys. . . . .	39
A2. The Range for Log $N_f$ Between the Two Chemical Environments Among Four Experimental Alloys. . . . .	40
A3. List of ANOVA Tables. . . . .	41
A4. ANOVA to Determine the Effect of Alloy Composition for Specimens Cycled at $\pm 12$ ksi (82.8 MPa) in the Oil Environment. . . . .	42
A5. ANOVA to Determine the Effect of Alloy Composition for Specimens Cycled at $\pm 18$ ksi (124.2 MPa) in the Oil Environment. . . . .	43
A6. ANOVA to Determine the Effect of Alloy Composition for Specimens Cycled at $\pm 12$ ksi (82.8 MPa) in the $3\frac{1}{2}\%$ Salt Water Environment . . . . .	44
A7. ANOVA to Determine the Effect of Alloy Composition for Specimens Cycled at $\pm 18$ ksi (124.2 MPa) in the $3\frac{1}{2}\%$ Salt Water Environment . . . . .	45

LIST OF TABLES (Cont'd)

TABLE	PAGE
A8. ANOVA to Determine the Effect of Environment for Specimens Cycled at <u>+12</u> ksi (82.8 MPa) . . . . .	46
A9. ANOVA to Determine the Effect of Environment for Specimens Cycled at <u>+18</u> ksi (124.2 MPa) . . . . .	47

## LIST OF ILLUSTRATIONS

FIGURE	PAGE
1. Test Specimen Geometry. . . . .	6
2. Effect of Cyclic Load Amplitude on Weibull Shape Parameter for the Ten Experimental Alloys Cycled in an Oil Environ- ment. . . . .	9
3. Effect of Purity on Notched Fatigue Life for Specimens Cycled in an Oil Environment. . . . .	16
4. Typical Slant Fracture Appearing in Zirconium Bearing Specimen ( $K_t=3.0$ ) Cycled at $\pm 12$ ksi (82.8 MPa) in an Oil Environment . . . . .	17
5. The Importance of Test Environment on the Notched Fatigue Life. . . . .	20
6. The Interaction Between the Test Environment and Dispersoid Type on the Notched Fatigue Life. . . . .	22
7. Stage I F.C.G. Initiation Areas: (a) Alloy A1, (b) Alloy C1, (c) Alloy E1. Magnification: 160X . . . . .	24
8. Overall View of Notched Fatigue Fracture Surfaces: (a) Alloy A1, (b) Alloy C1, (c) Alloy E1. Magnification 10X. .	26
A1. Schematic Diagram Illustrating the Analysis of Variance .	38

## SECTION I

### INTRODUCTION

In the past, two metallurgical approaches have been considered for improving the fatigue resistance of high strength aluminum alloys used by the aerospace industry. One approach is to reduce the volume fraction of large incoherent intermetallic particles such as  $\text{FeAl}_3$ ,  $\text{Cu}_2\text{FeAl}_7$ ,  $\text{Fe}_3\text{SiAl}_{12}$ ,  $\text{Fe}_2\text{Si}_2\text{Al}_9$ ,  $\text{Mg}_2\text{Si}$  (i.e. constituent particles). The second approach involves using a multiple step thermo-mechanical processing (TMP) rather than a simple warm aging for the final heat treatment (FTMT). Prior to 1973, the S-N curve for a material in either the notched or smooth ( $K_t = 1$ ) condition was the standard by which improvements were measured. Unfortunately, the myriad of test conditions and alloys used to investigate the importance of TMP between various investigators, References 1-7 , led to contradictory results. For example, different studies considered "high purity" alloys to be at different levels of iron plus silicon content. This confounds the comparison between the effect of purity and TMP where the variation in purity may have influenced the TMP results.

Since that time, with changing design philosophies, where a pre-existing flaw is assumed in all fracture critical structural components, the constant amplitude fatigue crack growth test has become more important. For this same reason the notched fatigue test is more important than the smooth fatigue test because it is a simple discriminator for fatigue crack growth. This argument is particularly strong when the notched fatigue life is greater than  $10^5$  cycles. The initial plastic deformation and not crack growth primarily determines the total fatigue life in the low cycle fatigue regime ( $N_f \leq 10^4$  cycles).

One purpose of this investigation is to consider the importance of purity in the notched fatigue behavior of axially loaded specimens. The alloys used in the present work had purity levels ranging from ultra-high purity levels (0.03 w/o Fe+Si), to those more typically found in the 7075 alloy produced in the 1970's (0.35 w/o Fe+Si max allowable in 7175; see Table I). In addition, this investigation is to assess the importance of the zirconium dispersoid on the notched fatigue behavior. The substitution of the normal chromium dispersoid for zirconium has been the partial basis for the development of the new alloy 7050.

Finally, the synergistic effect between the alloy's fatigue crack propagation and its corrosion resistance must be considered. The fatigue crack growth rate of aluminum alloys is dramatically influenced by the chemical environment in which the test is run, References 14, 15, 16 . There are two aspects to corrosion fatigue. First, fatigue loading can cause the activation of corrosion mechanisms which otherwise would remain dormant in a corrosion resistant alloy/temper combination. Or second, a corrosion sensitive alloy/temper can be aggravated by fatigue loading. In either case, the effects of alloying on the notched fatigue life must be judged in light of the fatigue test environment.

## SECTION II

### EXPERIMENTAL PROCEDURE

#### A. MATERIAL

Ten different alloys based on the 7075 composition were utilized in the present investigation to study two metallurgical variables: purity level and dispersoid type. Their compositions are given in Table 1 along with the composition limits of 7175 and 7050. Five of the alloys had a zirconium dispersoid (A1, B1, C1, D1, E1) while the other five alloys contained the normal chromium dispersoid (A, B, C, D, E). It should be noted that 7050 differs from 7175 in that the zirconium dispersoid replaces the chromium while the copper and zinc levels increase and the magnesium level decreases. The tramp elements of iron, silicon, manganese, and titanium are also held at slightly lower levels in 7050. In no case are any of the experimental zirconium bearing alloys within the specification limits of 7050 due to their low copper level (1.5 w/o). Therefore, one must be cautious in making conclusions about the 7050 alloy from the results of this study. Finally, 7175 is a higher purity version of 7075 which is a forging alloy. Although alloy E has the same purity level as 7175, their properties cannot be directly compared since E is a plate product. All ten alloys were heat treated to the T651 condition. These same alloys were previously used in other AFML investigations (References 8-12). These studies related how the constituent, dispersoid and hardening particles control the monotonic tensile, corrosion, stress-corrosion, and fracture toughness properties.

#### B. TESTING

As mentioned in the introduction, the notched fatigue test was used as a simple discriminator for fatigue crack growth resistance. The details of the

TABLE 1. COMPOSITION OF EXPERIMENTAL AND COMMERCIAL ALLOYS

COMPOSITION	7175	A	B	C	D	E
Zn	5.1-6.1	5.89	5.91	5.93	5.93	5.94
Mg	2.1-2.9	2.19	2.42	2.39	2.35	2.36
Cu	1.2-2.0	1.50	1.58	1.60	1.64	1.63
Cr	0.18-0.30	0.21	0.22	0.21	0.21	0.21
Fe	0.20	0.02	0.05	0.08	0.13	0.20
Si	0.15	0.01	0.02	0.04	0.06	0.11
Mn	0.10	<.01	<.01	<.01	<.01	<.01
Ti	0.10	.004	.005	.012	.012	.009
OTHERS(TOTAL)	0.15	<.01	<.01	<.01	<.01	<.01

COMPOSITION	7050	A1	B1	C1	D1	E1
Zn	5.7-6.7	5.73	5.68	5.84	6.02	5.98
Mg	1.9-2.6	2.39	2.31	2.31	2.33	2.45
Cu	2.0-2.8	1.50	1.51	1.54	1.51	1.52
Zr	0.08-0.15	0.12	0.12	0.12	0.12	0.12
Fe	0.15	0.01	0.04	0.08	0.11	0.20
Si	0.12	0.01	0.02	0.04	0.05	0.09
Mn	0.10	<.01	<.01	<.01	<.01	<.01
Ti	0.06	.0004	.005	.006	.005	.006
Cr	0.04	<.01	<.01	<.01	<.01	<.01
OTHER(TOTAL)	0.10	<.01	<.01	<.01	<.01	<.01

notched round specimen geometry with a  $K_t$  of three is given in Figure 1. To assure that the test results would not be biased by residual stresses introduced during machining, low stress grinding conditions were used (Reference 13).

Rather than trying to generate an entire S-N curve for all ten alloys, sufficiently low loads were used to assure that fatigue lives greater than 10,000 cycles were obtained. In this way, as explained in the introduction, the notched fatigue test is biased to ensure that most of the fatigue life is spent in crack propagation. In addition, as a large dispersion in the total number of cycles to failure is commonly found in low-load, long-life fatigue tests, only two load levels were used in these experiments. In this manner, it was economically feasible to run enough tests to obtain a sufficiently precise measure of the mean  $N_f$  to establish statistically significant trends.

In order to study the synergistic effect between an alloy's fatigue crack propagation behavior and its corrosion resistance, specimens were tested in an inert and an aggressive environment. A low sulfur vacuum-pump oil environment was used to insure that the known influence of water vapor present in laboratory air is minimized as water has a low solubility in oil. Salt-water (3½% NaCl) rather than pure water was chosen as the corrosive environment since the former is a more aggressive environment. This choice was made because the tests were run on a two ton (17.8 KN) Schenck fatigue machine where relatively high test frequencies are used (2000 cpm). Thus the time during which corrosion can occur is relatively short. To test for a corrosion-fatigue interaction, a sufficient amount of corrosion must be possible during the fatigue test. Thus, the more aggressive environment was chosen.

Previous work at AFML, Reference 4, found that a high purity 7075 alloy had a higher notched fatigue strength than a commercial purity 7075 alloy. Both alloys were also tested in a two ton (17.8 KN) Schenck fatigue machine with a zero mean load, i.e.,  $R=-1$ . In order to more precisely determine at what purity level

# NOTCHED FATIGUE SPECIMEN, $K_t=3$

AFML/LLS (OCT, '75)

THESE SURFACES FLAT AND PARALLEL WITHIN 0.0005  
AND SQUARE TO PITCH LINE OF THREAD.

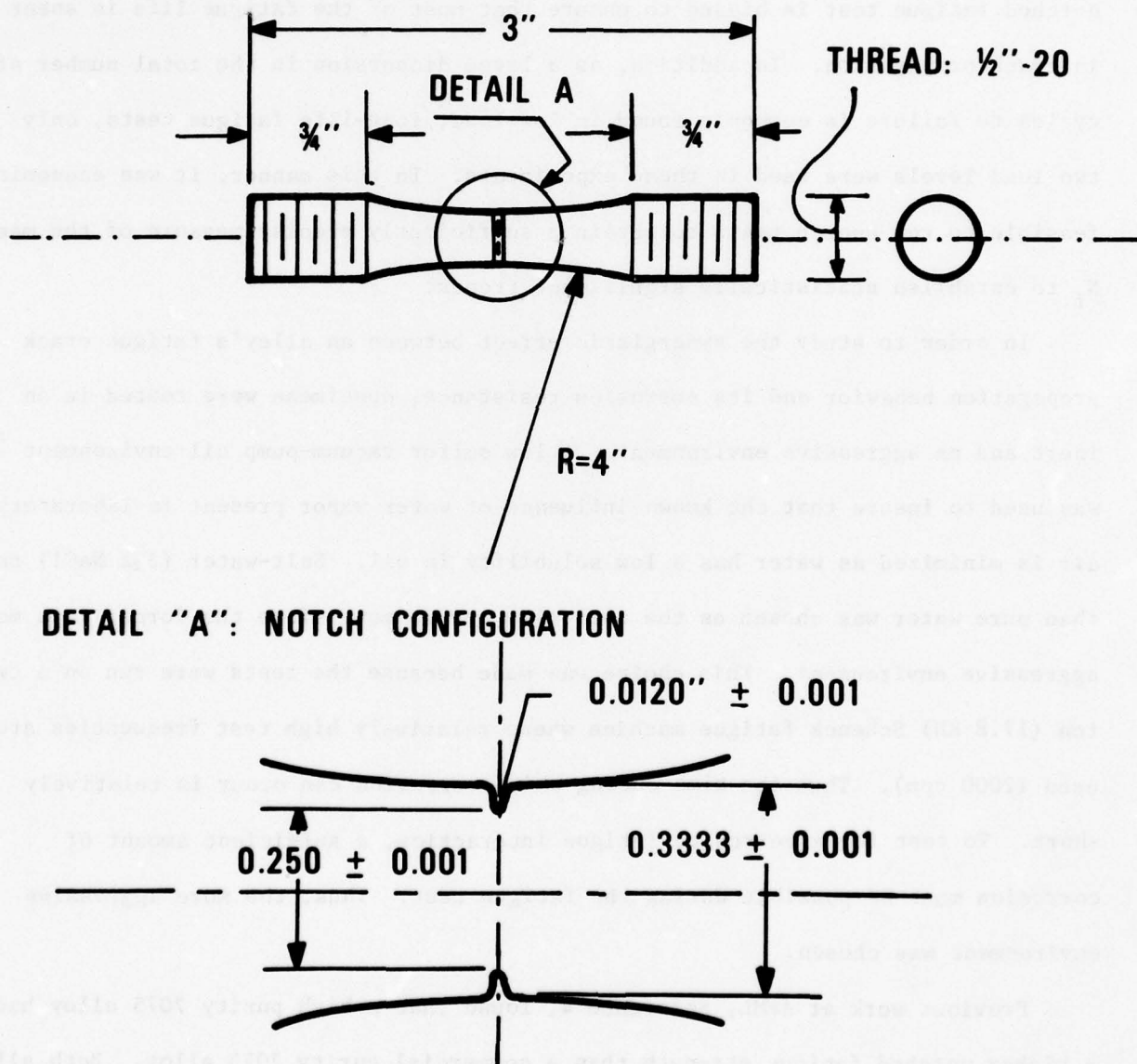


FIGURE 1: TEST SPECIMEN GEOMETRY

improved notched fatigue strength is increased for this R ratio the present tests were also run with completely reversed loading. However, the compressive part of the cycle causes the fracture surfaces to contact one another and obliterate the as-fractured topography. To allow a fractographic investigation of the role intermetallic particles play in fatigue fracture, a number of ancillary tests were run with a positive R-ratio (0.1).

### SECTION III

#### RESULTS

##### A. DATA ANALYSIS

A factorial design-of-experiment (see Appendix A) was chosen to answer the question of whether there is a synergistic effect between the ten different alloys and the two environments used. The analysis of this experimental design is the analysis of variance (ANOVA) which not only determines if a statistically significant interaction occurs between any combination of test variables, but also which of these interactions are more important.

Before performing an analysis of variance, a computer program, Reference 17, was used to fit the data in each test cell to a Weibull distribution. The Weibull probability density function is given by:

$$P(N) = \frac{bN^{b-1}}{\theta^b} \exp \left[ -\left(\frac{N}{\theta}\right)^b \right] \quad (1)$$

where  $b$  is the shape parameter and  $\theta$  is the location parameter. Since five replicate tests are insufficient to accurately define the tails of the distribution curve, the more complex form of the Weibull distribution with the guaranteed life was not used. It was found that with five data points for a least squares fit, it is possible to obtain a negative value for the guaranteed life parameter. A plot of cyclic load vs. the Weibull shape parameter is given in Figure 2 for the specimens cycled in the oil environment. The shape parameter is plotted only if the correlation coefficient is greater than 0.9. With one exception the specimens of the ten alloys cycled at  $\pm 12$  ksi (82.8 MPa) had a shape parameter of less than two while the specimens of these same alloys cycled at  $\pm 18$  ksi (124.2 MPa) always had a shape parameter greater than two. This result suggests a difference in

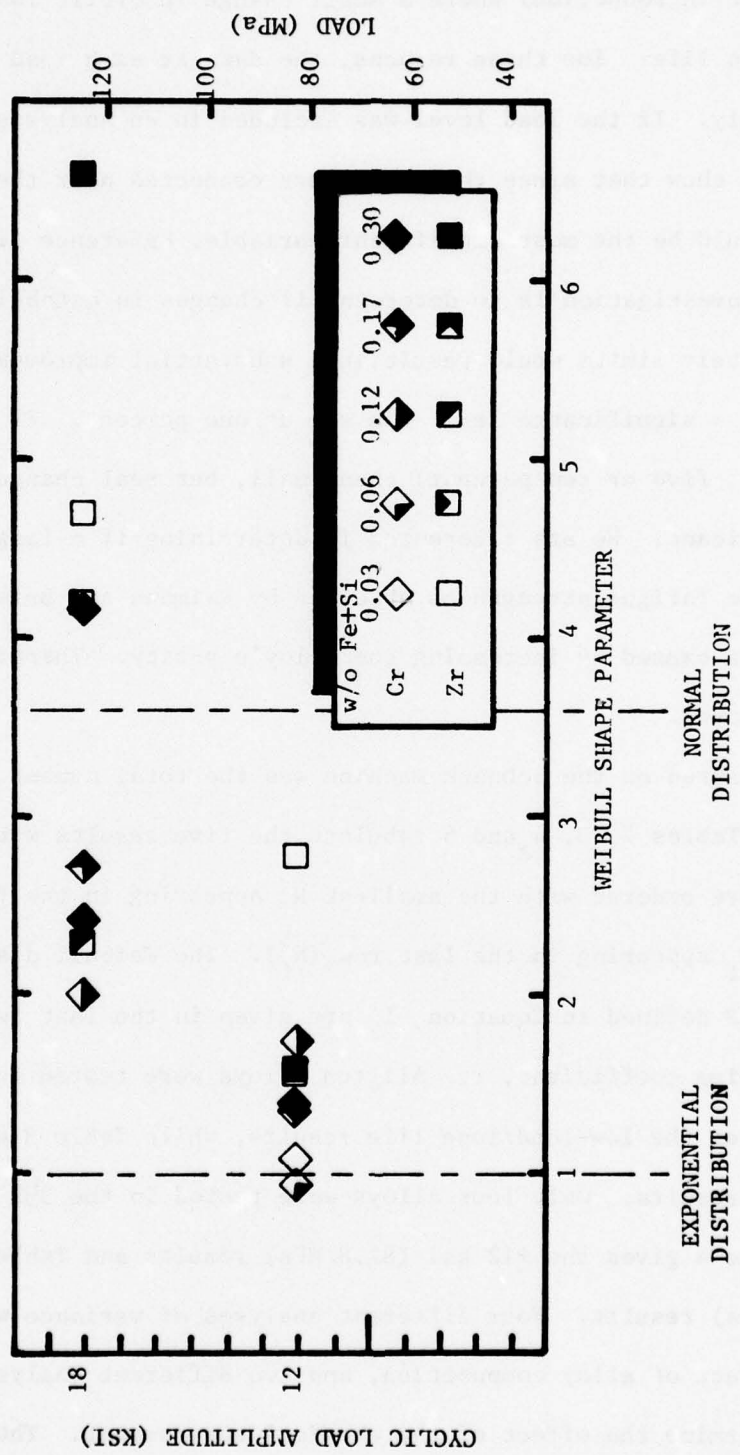


Figure 2. Effect of Cyclic Load on Weibull Shape Parameter for the Ten Experimental Alloys Cycled in an Oil Environment.

failure mechanism. In addition, the specimens were purposely tested near the fatigue limit (see Introduction) where a small change in cyclic load would produce a large change in life. For these reasons, the data at each load level were analyzed separately. If the load level was included in an analysis of variance the results would show that since the tests were conducted near the fatigue limit, the load level would be the most significant variable, Reference 18.

Since this investigation is to determine if changes in established alloy compositions or their limits would result in a substantial improvement in fatigue performance, the  $\alpha$  significance level was set at one percent. If the  $\alpha$  was made less severe (e.g., five or ten percent) then small, but real changes would be considered significant. We are interested in determining if a large (40%) improvement in the fatigue strength as observed by Reimann and Brisbane, Reference 4, was caused by increasing the alloy's purity. Therefore, the small value of  $\alpha$  was chosen.

The life measured on the Schenck machine was the total number of kilocycles-to-failure,  $N_f$ . Tables 2, 3, 4, and 5 tabulate the five results within each test cell. The data are ordered with the smallest  $N_f$  appearing in the first row ( $N_f^1$ ) and the largest  $N_f$  appearing in the last row ( $N_f^5$ ). The Weibull distribution parameters  $b$  and  $\theta$  defined in Equation 1 are given in the last two rows along with the correlation coefficient,  $r$ . All ten alloys were tested in the oil environment; Table 2 gives the low-load/long-life results, while Table 3 gives the higher-load/longer-life results. Only four alloys were tested in the 3½% salt water environment; Table 4 gives the +12 ksi (82.8 MPa) results and Table 5 gives the +18 ksi (124.2 MPa) results. Four different analyses of variance were made to determine the effect of alloy composition, and two different analyses of variance were made to determine the effect of the chemical environment. The details of these analyses are present in Appendix A, and the results are discussed in the next two sections.

TABLE 2. NOTCHED FATIGUE LIFE (KILOCYCLES) AND WEIBULL PARAMETERS OF EXPERIMENTAL ALUMINUM ALLOYS CYCLED AT  $\pm 12$  KSI (82.8 MPa) IN AN OIL ENVIRONMENT ( $R=-1$ ,  $K_t=3$ )

DISPERSOID TYPE	w/o Fe+Si	Cr				Zr				
		0.03	0.07	0.12	0.19	0.31	0.02	0.06	0.12	0.16
1	V*	N	V	N	N	V	V	N	S	N
	-	1771.1	971.7	972.1	246.8	671.3	1204.6	227.9	400.9	567.2
2	N	N	N	N	N	V	S	V	S	N
	193.8	3230.5	1329.9	2408.9	725.2	931.0	2220.3	387.8	793.6	574.1
3	N	N	N	N	N	N	V	S	S	V
	677.4	5325.6	1750.8	3075.3	800.1	1115.3	3939.5	465.1	1029.0	755.6
4	V	N	V	N	N	N	S	V	V	V
	1058.3	7048.8	3540.7	5415.1	1422.0	1574.7	4349.0	925.9	1460.1	1654.9
5	N	N	N	N	N	S	S	V	V	S
	2740.8	10900.6	7008.0	6290.8	4178.8	1600.9	6572.6	1044.8	2282.0	3857.5
AVERAGE	1167.6	5655.3	2920.2	3632.14	1474.6	1178.6	3657.2	610.3	1193.1	1481.9
r	.98	.97	.95	.99	.97	.98	.99	.98	.99	.88
θ	792.4	6557.9	3335.4	4294.3	1605.2	1336.4	4290.8	712.9	1388.2	1709.3
b	1.079	0.928	1.230	1.376	0.971	2.769	1.559	1.661	1.581	1.101

\*V = vee fracture    N = normal fracture    S = slant fracture

TABLE 3. NOTCHED FATIGUE LIFE (KILOCYCLES) AND WEIBULL PARAMETERS OF EXPERIMENTAL ALUMINUM ALLOYS CYCLED AT  $\pm 18$  KSI (OR 124.2 MPa) IN AN OIL ENVIRONMENT ( $R=-1$ ,  $K_t=3$ )

DISPERSOID TYPE	w/o Fe+Si	Cr						Zr					
		0.03	0.07	0.12	0.19	0.31	0.02	0.06	0.12	0.16	0.29		
1	N*	76.8	52.6	69.8	113.1	N	80.4	V	63.8	V	55.9	N	104.9
2	N	93.2	77.0	91.6	156.1	N	126.0	V	78.9	V	N	V	115.0
3	N	112.2	179.6	98.8	187.0	N	158.3	V	V	V	V	V	126.8
4	N	117.2	182.1	187.3	233.3	N	202.0	N	103.4	63.3	66.9	V	
5	N	147.9	188.7	217.2	306.8	N	252.6	S	V	V	N	N	127.5
AVERAGE		109.4	136.0	132.9	199.3	164.5	674.1	92.7	69.4	71.2	126.2		
r	.99	.86	.94	.99	.99	.72	.97	.97	.96	.93	.95		
θ	120.2	189.4	154.4	225.6	187.9	527.0	102.0	80.3	80.3	78.3	134.7		
b	4.148	1.388	1.999	2.711	2.423	5.059	4.199	1.535	4.189	6.582			

\*N = normal fracture, V = vee fracture, S = slant fracture

TABLE 4. NOTCHED FATIGUE LIFE (KILOCYCLES) OF EXPERIMENTAL ALUMINUM ALLOYS CYCLED AT +12 KSI (OR 82.8 MPa) IN A 3½% SALT WATER ENVIRONMENT (R=-1,  $K_t=3$ )

Cr/Zr w/o Fe+Si	Cr		Zr	
	0.07	0.19	0.06	0.16
1	N* 33.6	N 90.5	N 115.0	N 69.3
2	N 129.3	N 110.0	N 120.0	N 86.2
3	N 186.2	N 150.0	N 317.8	N 111.2
4	N 219.3	N 185.4	N 495.1	N 137.6
5	N 727.1	N 260.3	N 540.1	N 422.4
AVERAGE	259.1	159.2	317.6	165.3
r	.97	.97	.93	.88
θ	285.5	178.4	379.8	191.3
b	0.913	1.278	1.287	1.297

\*N = normal fracture, V = vee fracture, S =slant fracture

TABLE 5. NOTCHED FATIGUE LIFE (KILOCYCLES) OF EXPERIMENTAL ALUMINUM ALLOYS CYCLED AT +18 KSI (OR 124.2 MPa) IN A 3½% SALT WATER ENVIRONMENT  
(R=-1,  $K_t = \overline{3}$ )

Cr/Zr	Cr		Zr	
w/o Fe+Si	0.07	0.19	0.06	0.16
1	N* 9.9	N 9.8	N 18.8	N 13.2
2	N 22.9	N 13.4	N 19.8	N 14.8
3	N 32.2	N 14.4	N 20.8	N 18.1
4	N 38.7	N 20.9	N 31.0	N 21.7
5	N 40.5	N 22.2	N 34.3	N 21.9
AVERAGE	28.8	16.1	24.9	17.9
r	.96	.97	.89	.97
θ	34.4	18.2	28.0	19.6
b	1.711	2.997	3.324	4.436

\*N = normal fracture, V = vee fracture, S = slant fracture

### B. EFFECT OF ALLOY COMPOSITION

Under certain restricted conditions, the alloy's purity level was found to be the only significant metallurgical variable. First, for specimens tested in the 3½% salt water environment, neither purity level nor dispersoid type (or their interaction) significantly affected the number of cycles to failure. However, for specimens tested in the oil environment, the purity level did significantly effect the fatigue life, but only at the lower-load, longer-life regime. Figure 3 is a bar graph for the specimen cycled in the oil environment giving the average notched fatigue life for both cyclic loads as a function of purity. It should be noted that for the +12 ksi (82.8 MPa) test results, increasing the purity level does not continually increase the notched fatigue life. This fact requires further verification. The reasons for purity not being significant at high loads and in the 3½% salt water solution will be discussed in the next section.

Not all the specimens tested failed within the notched region. A number of specimens failed at a 45° angle outside the notched region. A typical example of this behavior is shown in Figure 4. All the specimens were identified as to the macroscopic fracture appearance as either: (1) normal failure (N), (2) slant fracture (S), or (3) vee fracture (V). The vee fracture fails within the notch plane except in the middle of this plane a single vee shaped protrusion lies across two-thirds of the specimen diameter. These fracture types are also recorded in Tables 2, 3, 4, and 5. As the grips were designed to insure that no torsion stress can be applied to the test specimen during mounting, the occurrence of the slant fracture or vee fracture is attributed to the presence of zirconium and not to poor testing procedure. A chi-square test, Reference 19, is used to determine if there was a correlation between the abnormal fracture morphology (V and S)

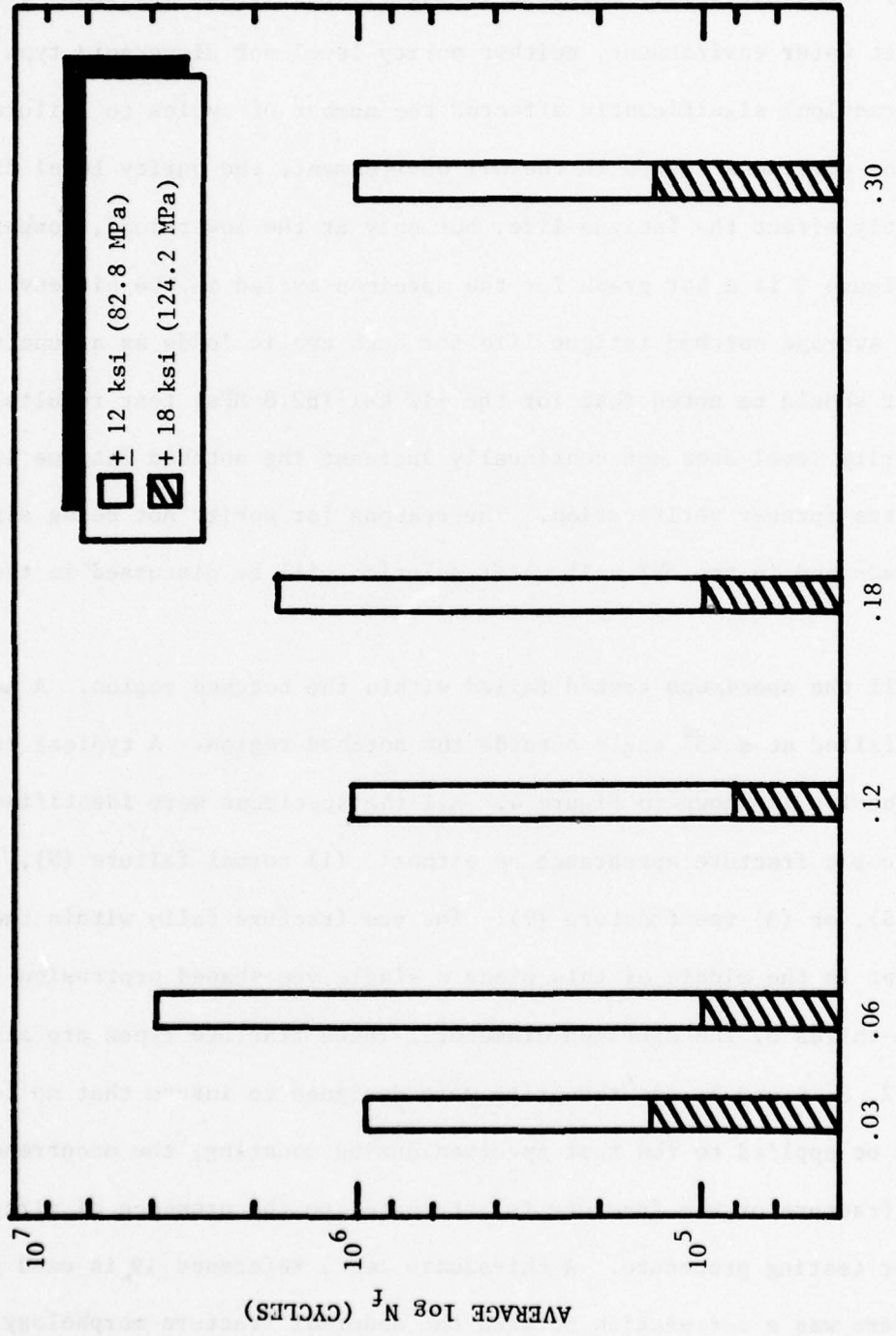


Figure 3. Effect of Purity on Notched Fatigue Life for Specimens Cycled in an Oil Environment.

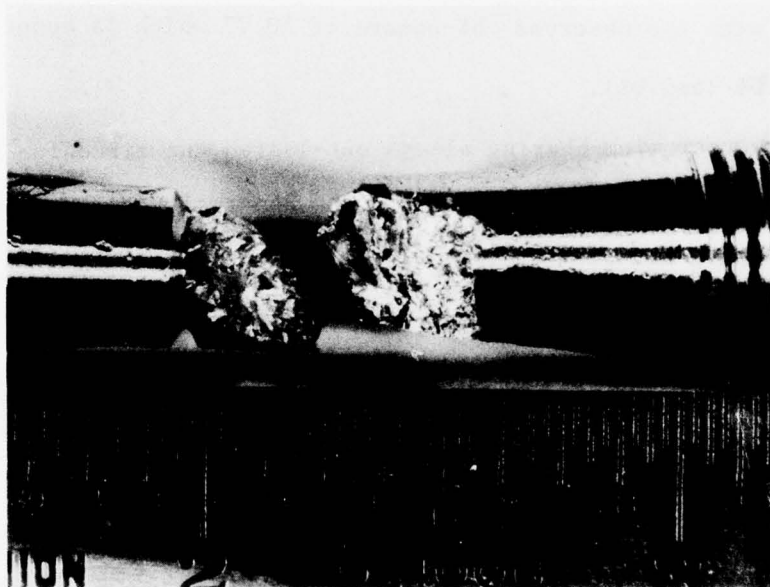


FIGURE 4. TYPICAL SLANT FRACTURE APPEARING IN ZIRCONIUM-BEARING SPECIMEN ( $K_T=3.0$ ) CYCLED AT  $\pm 12$  KSI (82.8 MPa) IN AN OIL ENVIRONMENT.

with the zirconium bearing alloys. Table 6 gives the contingency table used for this analysis. The data is only for specimens tested in the oil environment as the zirconium-bearing alloys did not fail abnormally in the 3½% salt water environment. The observed chi-square was calculated to be 27.28 which is nearly three times greater than the critical value of 9.21 ( $\alpha=0.01$ ). This analysis verified that unusual fracture behavior is associated with the zirconium dispersoid. A similar chi-square test was made to determine if the purity level is associated with the abnormal fracture morphology. The purity level was not found to be significant with the observed chi-square of 10.77 which is about half the critical value of 20.09 ( $\alpha=0.01$ ).

Since the chromium-bearing alloys out-lasting the zirconium-bearing alloys (3118.5 vs. 1830.9 kilocycles), the abnormal V and S fracture is associated with a shorter fatigue life. However, the ANOVA studies did not show the dispersoid type to be a significant variable because the small  $\alpha$  value was used to screen for more dramatic life increases on the transformed data ( $\log N_f$ ). A life increase on the order of four times (see Figure 3; purity levels of 0.03 w/o vs 0.06 w/o) is necessary before the variable is considered significant. The role dispersoid particles play in determining the notched fatigue life must be considered in terms of the test environment.

#### C. EFFECT OF CHEMICAL ENVIRONMENT

When the test environment is included as a variable in addition to the alloy composition in an analysis of variance, the importance of corrosion-fatigue is prominent. Figure 5 gives the average notched fatigue life for each test environment as well as the different dispersoid types and purity levels. It is clear that changing the test environment has the most effect on fatigue life. The

TABLE 6. FREQUENCY TABLE USED TO DETERMINE IF THERE IS A CORRELATION  
BETWEEN THE DISPERSOID TYPE AND THE MACROSCOPIC FRACTURE  
APPEARANCE

$\chi^2 = 27.28$ DISPERSOID TYPE	Cr	Zr	TOTAL
N(normal)	42	15	57
V (vee)	8	25	33
S (slant)	0	10	10
TOTAL	50	50	100

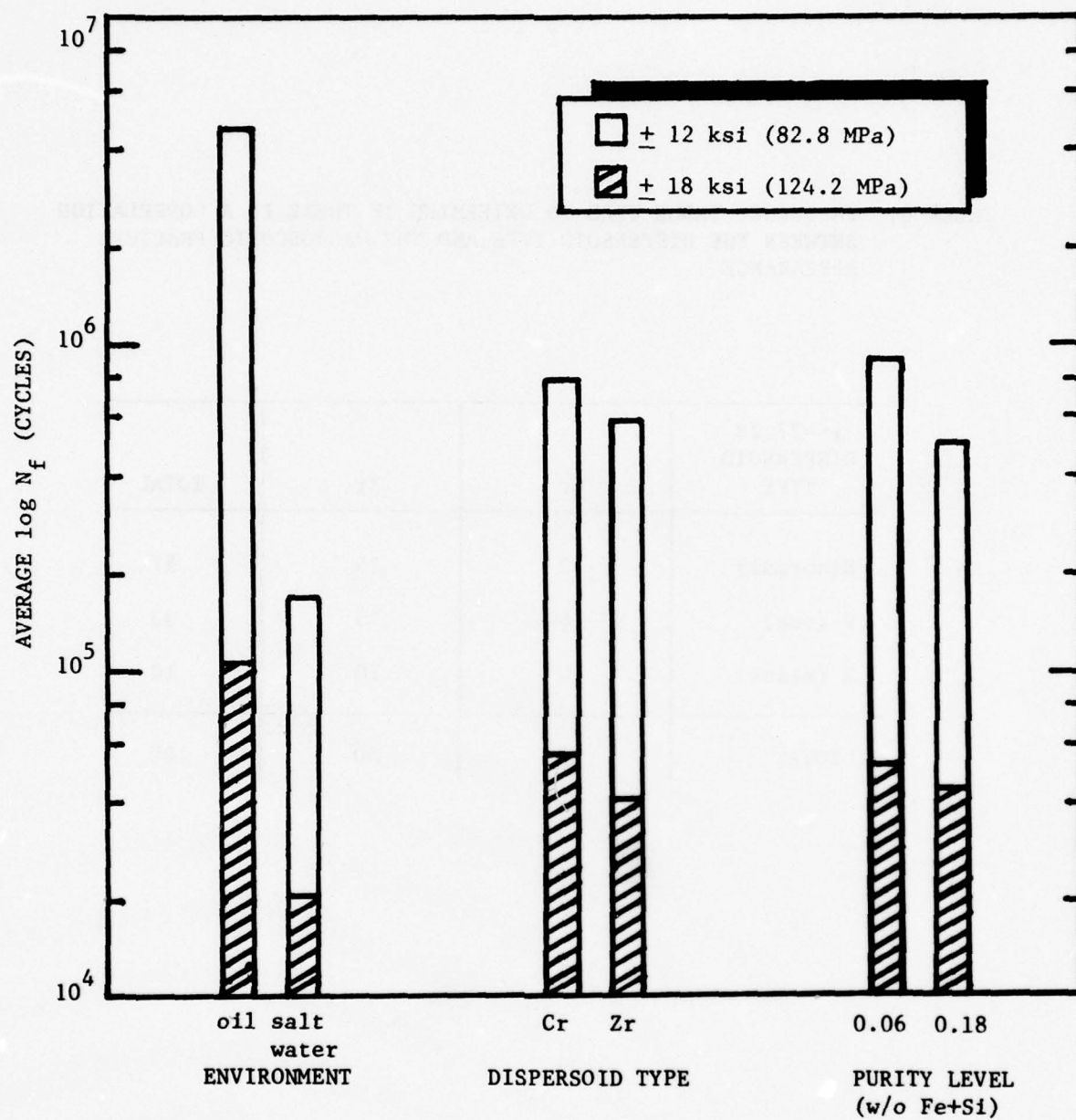


Figure 5. The Importance of Test Environment on the Notched Fatigue Life.

importance of environment, however, is not new. Rather, a short duration, environment-sensitive test lasting at most one and half days (3.5 million cycles at 2000 cpm) is new. This fact may be useful in designing alloy screening tests in the future.

Again, there is no dramatic effect in changing the dispersoid from chromium to zirconium. At both cyclic load levels, the zirconium-bearing specimens exhibit a slightly shorter fatigue life. This is consistent with the previous analysis, the specimens which did not fail completely within the notch plane have a shorter fatigue life. However, one point which is not obvious from Figure 5 is the strong interaction between the environment and dispersoid type for the specimens tested at the shorter-life/higher-load which disappears at the longer-life/lower-load test conditions. To see this effect, the center pair of cross hatched bars must be further broken down into the results for each environment. This is done in Figure 6 which shows that there is no difference in the notched fatigue lives between the chromium-bearing and zirconium-bearing alloys tested in the salt water environment. The small difference observed in Figure 5 is due to the specimens tested in the oil environment. This same interaction does not occur for specimens tested at the longer-life/lower-load because in this region purity level, not dispersoid type, becomes more important as previously discussed and illustrated in Figure 3. The importance of purity level at the  $\pm 12$  ksi (82.8 MPa) but not at  $\pm 18$  ksi (124.2 MPa) is the same for the intermediate purity levels tested in 3½% salt water as found for all five purity levels tested in oil. This fact is illustrated by the last pair of bars in Figure 5.

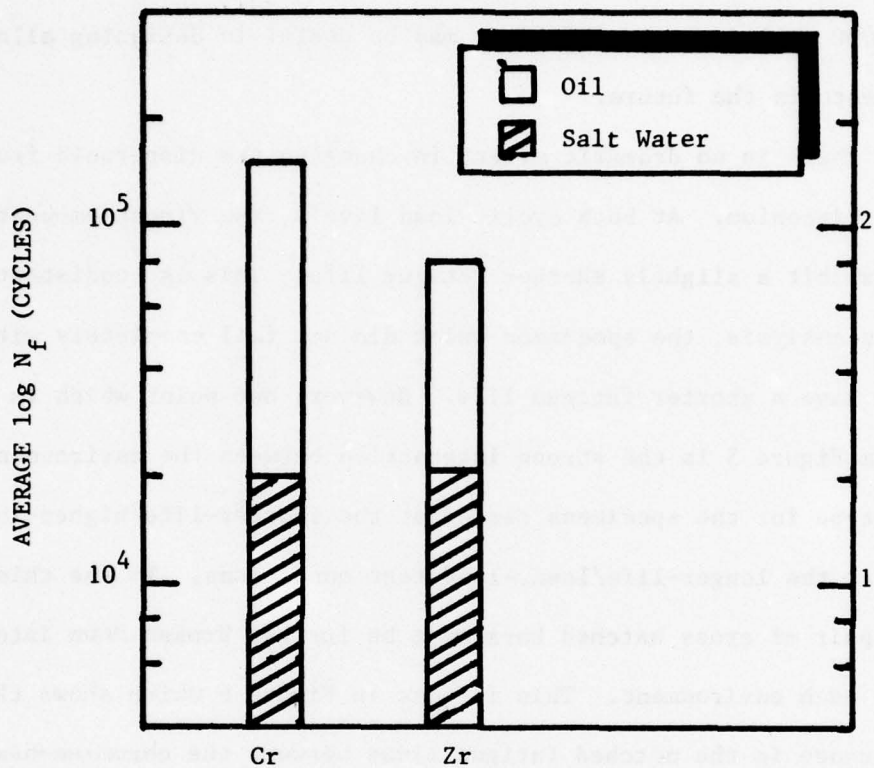


Figure 6. The Interaction Between Test Environment and Dispersoid Type on the Notched Fatigue Life

#### D. ANCILLARY FRACTOGRAPH STUDIES

As all the data analyzed were from specimens which saw completely reversed loading, the fracture surfaces were obliterated making it difficult to interpret topographic features. For this reason, a number of tests were run where no compressive loads were applied to the specimens. The zirconium-bearing alloys tested in oil at  $\pm 12$  ksi (82.8 MPa) which had exhibited the slant  $45^\circ$  failure mode were chosen for study. Three purity levels were considered (0.02, 0.12, 0.29 w/o Fe+Si) as purity was the only significant variable for specimens tested in the oil environment at the lower cyclic load. Three replicate tests were run with a cyclic load of 22.5 ksi (155.3 MPa) and R=0.1. The average cyclic life was 475.1, 161.1, and 100.7 kilocycles in order of decreasing purity. The specimens which had the smallest difference in life from the cell average were chosen for fractographic study.

None of the specimens tested with only tensile loading had either the vee or slant macroscopic fracture surface. This fact was rather surprising in that 80% of the zirconium-bearing alloys cycled at nearly the same cyclic load (24 ksi or 165 MPa) but R=-1 had a slant fracture. As the hardening precipitates formed during the standard T651 heat treatment of 7075 are shearable by dislocations there is a tendency to have inhomogeneous slip band formation. Precision metallographic sectioning of specimens with the slant fracture has verified that the slip bands are parallel to the fracture surface, Reference 20 . Apparently, sustained crack growth by this fracture mode is more likely when completely reversed loading rather than tensile loading is applied to the experimental alloys. Interestingly enough, fractographs, Figure 7, of all three alloys tested using only cyclic tensile loads show areas of flat featureless planar cracking near the notch root. These fractographs also suggest that there may be an influence of the alloy's purity on this mode of crack propagation. Figure 7a is a representative area for the ultra-high-purity alloy (A1) showing many areas with this fracture mode. However,



Figure 7. Stage I F.C.G. Initiation Areas: (a) Alloy Al, (b) Alloy C1, (c) Alloy E1.  
Magnification: 160X

the less pure alloys (C1, E1) show fewer and fewer areas containing Stage I cracking (Figures 7b and 7c, respectively).

As can be seen from the low magnification fractographs in Figure 8, not only crack initiation but also crack propagation is affected by the purity of the alloy. As marked in Figure 8, the crack initiation occurred over one-fourth of the notched circumference for the purest alloy while for the other two alloys initiation occurred over approximately one-third of the notched circumference. These results are consistent with crack initiation studies on other aluminum alloys, Reference 21. These investigators had found that the largest incoherent constituent particles found in 2024 were preferential initiation sites. When the number of these sites was decreased by the use of 2124, the crack initiation process was changed to the intense slip bands which form in both these alloys when they are naturally aged.

The fact that Stage II crack propagation is influenced by purity is deduced by the shape of the fast fracture region in Figure 8. It can be seen that nearly three-quarters of the ultra-high-purity alloy has nearly three-quarters of its circumference containing the final fast fracture region. In Figure 8b, for the medium-purity alloy used in this study, only half of the circumference intersects the fast fracture region, but a very irregular crack front is marked by the tensile overload. The low-purity alloy in this study behaves like the medium-purity alloy except that the crack front appears more uniform, Figure 8c. In the ultra-high-purity alloy, the fatigue crack propagates radially from the initiation area which is dominated by Stage I cracking. This produces a longer crack front than found in the other two alloys. For the medium-purity alloy, the crack does not grow radially from the Stage I crack growth area but grows locally faster or slower so that prior to the final fast fracture, a sinusoidal crack front is present. By decreasing the alloy purity, these local discontinuities occur with sufficient

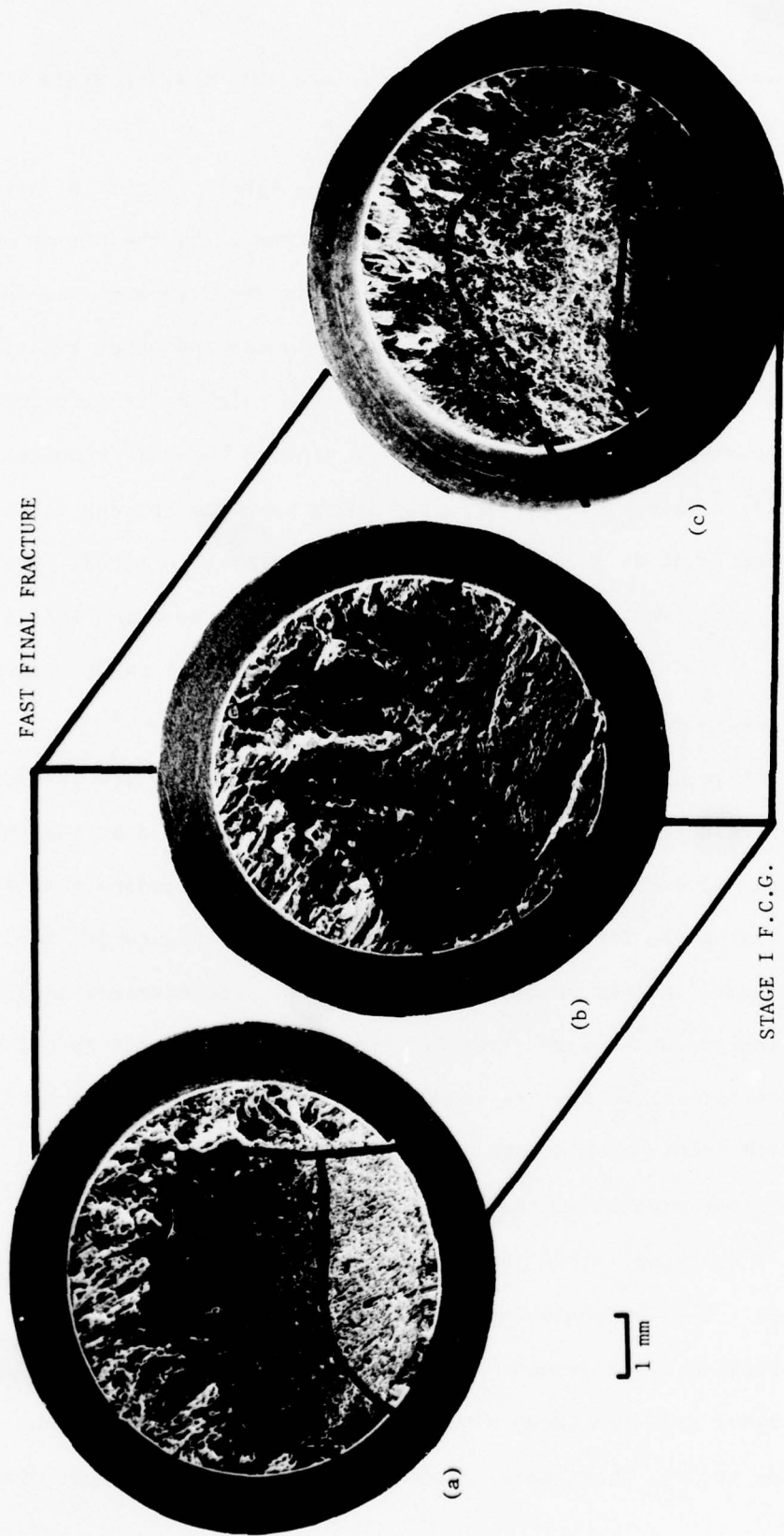


Figure 8. Overall View of Notched Fatigue Fracture Surfaces: (a) Alloy Al, (b) Alloy C1,  
(c) Alloy El. Magnification: 10X.

frequency so as to make the crack front appear straight at low magnification as shown in Figure 8c. Between the Stage I crack growth area and the fast final fracture area is the region of Stage II crack growth. The five times shorter fatigue life for alloy El may be partially attributed to Stage II crack propagation resistance of alloy Al. Since the fatigue life of the notched specimens is composed of both Stage I and Stage II fatigue crack growth, this tentative conclusion must be verified by fatigue crack propagation tests.

## SECTION IV

### DISCUSSION

To test the hypothesis that a large improvement (40%) in the notched fatigue strength of aluminum alloys can be obtained by increasing their purity level, a small alpha level was chosen. If purity levels would substantially increase the fatigue strength, then purity would be found to be significant by the analysis of variance with a severe criterion. The results of this study do not completely substantiate the results of the Reimann-Brisbane study, Reference 4. While it is true that purity level is significant at the 99% confidence level, it is only significant for limited test conditions. First, purity does not significantly affect the fatigue life in an aggressive 3½% salt water environment at the load levels tested. This may be due to the fact that not all the purity levels were tested in the aggressive environment. Second, purity was only significant at the lower load tested in the inert oil environment. As the Reimann-Brisbane tests were conducted in laboratory air where the relative humidity is nominally between 40-65%, the severity of their test environment lies between the two environments used in the present study. This fact suggests that the alloys' purity level should be important in the inert environment at both load levels tested. This observed discrepancy can possibly be explained by the Weibull shape factor. It was shown to be different for each cyclic load level tested in the present investigation. As discussed earlier (Section III.A.), this suggests that a change in the failure mechanism has occurred. Unfortunately, these specimens were loaded in compression and the fracture surfaces were obliterated so that this hypothesis could not be verified using fractography.

Even though the statistical analysis proves there is a significant difference in the notched fatigue life among the five purity levels, unexpectedly the graph in Figure 3 shows no systematic increase in life with increasing purity. Broken test specimens were sectioned, polished and compared with 3-D motifs for the ten alloys to verify that they were all machined with the tensile axis parallel to the rolling direction. No discrepancies were noted. In addition, a chemical analysis was run on selected specimens for the elements of iron, silicon, zirconium, and chromium to check if the samples were mislabeled. Again no discrepancies were noted. The measured percent bending stress of the Schenck fatigue machine is less than seven percent. This consistently good alignment eliminates test method.

There are two possible explanations for both the erratic relationship between alloy purity level and notched fatigue life when  $R=-1$ , and the decrease in life with increasing purity at a cyclic stress amplitude of 24 KSI (165.6 MPa) when  $R=-1$ , but not when  $R=0.1$ . Energy dispersive analysis done on an electron microprobe verified that many of the large intermetallic particles contained not only iron and silicon but also copper and magnesium, Reference 18. Since all the alloys tested had a constant amount of copper and magnesium (Table 1), different amounts of these elements can: (1) combine with the available iron and silicon, (2) precipitate as metastable precipitates during heat treatment, or (3) the excess forms a stable intermetallic. Thus, using the w/o Fe+Si alone as a measure for the volume fraction of large intermetallic particles can explain the unexpected absence of correlation between w/o Fe+Si and the notched fatigue life when  $R=-1$ .

Previous work, Reference 8, showed that the alloys with the T651 heat treatment had two to five times larger area percent of impurities than the same alloys given a different heat treatment. This result is not consistent with the microstructures shown in Reference 8 where it appears that the volume fraction of the coarse intermetallic particles should be about the same for both heat treatments, as

expected, Reference 25. This apparent discrepancy may be due to the criteria whereby "contrast threshold settings were adjusted carefully". This hypothesis is based on the fact that the peppered bands for the TMP microstructures shown in Reference 8 are generally absent in the T651 microstructures. These peppered bands are associated with selective attack on smeared surfaces caused by a galvanic cell consisting of the specimen and the iron tongs holding the mount during the etching, Reference 18. Since the TMP heat treated alloys have a lower strength, Reference 10, more disturbed areas are expected for alloys of this heat treatment, though disturbed areas are also visible in Reference 8 for the alloys in even the peak hardened condition, T651. Thus, the linear agreement between area percent impurities and w/o Fe+Si for even the highest purity alloys is fortuitous.

The increasing notched fatigue life (at  $\pm 12$  KSI, 82.8 MPa) with increasing purity at  $R=0.1$  (Figure 3) can also be explained in metallurgical terms. The hardening precipitates ( $n'$ ) for 7075-T651 are shearable by dislocations and inhomogeneous slip bands concentrate the deformation to a small volume of material. When completely reversed loading is used,  $R=-1$ , it is possible that different dislocation sources become active to accommodate the imposed plastic strains at the crack initiation sites. When repeated tensile loading is used,  $R=0.1$ , the plastic strain is accommodated primarily by dislocation multiplication along the initially weakened planes.

Another equally plausible explanation of the experimental results is based in mechanical terms, and involves the importance of the notch machining process. First, the notches were carefully machined into the alloys by stress-free grinding procedures, Reference 13. However, after the testing program was underway an AFML study on surface integrity of machined materials, Reference 24, was found which quantified this question. It gave evidence that the fatigue strength

(R=-1, cantilever bendings) in 7075-T7351 is very sensitive to surface grinding. Data shows that gentle grinding gives a fatigue strength of 24 ksi (166 MPa) while abusive grinding gives a fatigue strength of 9 ksi (62 MPa). On the other hand in this same report, other surface finishes produced by disk sanding, turning, chemical machining, or end mill peripheral cutting do not change the fatigue strength significantly. Since the notch was ground into the specimen tested in the present program, it appears possible that part of the experimental scatter and the decrease in fatigue life may be explained by the effect of machining. Unfortunately, even with strict grinding specifications it is possible in the present experiment that different alloys were machined by different machinists or the same machinist at different times with slight but systematic deviations from the printed specification. Thus, future notched fatigue programs should require: (1) specify that the specimens are machined at random if grinding is used, or if economically feasible, (2) prohibit grinding in machining the notch. Further testing is required to determine if the purity level or the machining is responsible for the anomalous behavior at the highest purity level tested.

Although the reported slant fracture (see Figure 4) occurred at the low cyclic loads, the origin of this fracture mode appears to be metallurgical. A chi-square analysis showed a strong correlation between the appearance of the slant or vee fracture and the zirconium-bearing alloys irregardless of their purity level. Interestingly, this type of failure mode does not dramatically affect the fatigue life as one might fear whenever inhomogeneous plastic flow occurs. For this reason the dispersoid type used in the alloys was not found significant with the small alpha used in this study.

Tests lasting less than one and a half days surprisingly provided sufficient time for the aggressive environment of 3½% salt water to significantly affect the notched fatigue life. Despite the fact that the chromium-bearing alloys experience

a less uniform and deeper exfoliation corrosion than the zirconium-bearing alloys, Reference 12, the chromium-bearing alloys out-lived the zirconium-bearing alloys at both cyclic load levels tested. To explain these unexpected results, it is hypothesized that if the cycling were done at a lower frequency to allow time for more corrosion to occur during the test, then the exfoliation resistant zirconium-bearing alloys could out perform the chromium-bearing alloys in a corrosion-fatigue environment.

## SECTION V

### CONCLUSIONS

Based on the results of the present investigation, the authors made the following conclusions.

- (1) Specifying higher purity limits will not significantly improve (by 40%) the notched fatigue strength of commercial 7075-T651 in normal service environments.
- (2) Replacing the normal 7075 grain refiner of chromium by zirconium will slightly decrease the notched fatigue strength of these alloys. This effect is not significant at the one percent significance level chosen for this study.

## REFERENCES

1. Thompson, D.S., S.A. Levy, G.E. Spangler and D.K. Benson, Program to Improve the Fracture Toughness and Fatigue Resistance of Aluminum Sheet and Plate for Aircraft Applications, AFML-TR-73-247, Vol. I, (September 1973).
2. McEvily, A.J., J.B. Clark and A.P. Bond, "Effect of Thermal Mechanical Processing on the Fatigue and Stress Corrosion Properties of an Al-Zn-Mg Alloy", Trans. ASM 60, pp. 661-71 (1967).
3. Ostermann, F., Improved Fatigue Resistance of Al-Zn-Mg-Cu (7075) Alloys Through Thermomechanical Processing, AFML-TR-71-121 (September 1971).
4. Reimann, W.H. and A.W. Brisbane, "Improved Fracture Resistance of 7075 Through Thermomechanical Processing", Eng. Fracture Mech. 5, pp. 67-78 (1973).
5. Titchener, A.L. and C.D. Ponniah, "The Effect of Thermomechanical Treatment on the Fatigue Behavior of an Al-Mg-Si-Mn Alloy", Proc. 3rd Int. Conf. Strength of Metals and Alloys, Cambridge, Vol. I, pp. 432-36 (1973).
6. DiRusso, E., M. Conserva, F. Gatto and H. Markus, "Thermomechanical Treatments on High Strength Al-Zn-Mg-Cu Alloys", Met. Trans. 4, pp. 383-86 (1973).
7. Hyatt, M.V., Program to Improve the Fracture Toughness and Fatigue Resistance of Aluminum Sheet and Plate for Airframe Applications, AFML-TR-73-224 (September 1973). \*
8. Blau, P.J., "Observations on the Distribution of Iron and Silicon Particles in a High-Strength Aluminum Alloy", "Metallography", 1, (1975) pp. 187-201.
9. Effect of Iron and Silicon Content on Stress Corrosion Cracking in a Thermomechanically Processed Aluminum Alloy, AFML-TR-75-215, Air Force Materials Laboratory Technical Report, (March 1976). \*
10. Influence of Iron and Silicon Content on the Tensile Properties of 7x75 and Zr-Modified 7x75 Aluminum Plate, AFML-TR-75-140, Air Force Materials Laboratory Technical Report (October 1975). \*
11. "Effect of Iron and Silicon Content on the Fracture Toughness of 7x75 and Zr-Modified 7x75 Aluminum Plate", TM-LL-75-10, Air Force Materials Laboratory Technical Memorandum, (July 1975).
12. Effects of Purity and Processing on the Exfoliation Corrosion Behavior of 7x75 Aluminum Plate, AFML-TR-75-43, Air Force Materials Laboratory Technical Report, (July 1975). \*

13. Private communications, William Mast, MetCut Research Associates, Inc., 3980 Rosslyn Drive, Cincinnati, Ohio 45209, November 4, 1975.
14. Truckner, W.G., Staley, J., Bucci, R. and Thakker, M., Effect of Microstructure on Fatigue Crack Growth of High-Strength Aluminum Alloys, Air Force Materials Laboratory Technical Report, AFML-TR-76-169, December 1976.\*
15. Wei, R.P., "Some Aspects of Environment Enhanced Fatigue Crack Growth", Eng. Fracture Mech., 1, (1970) p. 633.
16. Hudson, C.M. and Sewars, S.K., "A Literature Review and Inventory of the Effects of Environment on the Fatigue Behavior of Metals", Eng. Fracture Mech., 8, (1976), p. 315.
17. Hewlett-Packard Calculator Model 9100A Program Library, No. 70810, Weibull Distribution Parameter Calculation for Failure Data, (1968).
18. Santner, J.S., unpublished research, Air Force Materials Laboratory.
19. Natrella, M.G., Experimental Statistics, National Bureau of Standards Handbook 91, October 1966, U.S. Government Printing Office, Washington, D.C.
20. Eylon, D. and J.S. Santner, unpublished research, Air Force Materials Laboratory.
21. Fine, M.E., private communications, Northwestern University.
22. Eisenhart, C., "Assumptions Underlying the Analysis of Variance", Biometrics, 3, (March 1947) pp. 1-21.
23. Bartlett, M.S., "The Use of Transformations", Biometrics, 3, (March 1947) pp. 39-52.
24. Surface Integrity of Machined Materials, AFML-TR-74-60, Air Force Materials Laboratory Technical Report, (April 1974).\*
25. A Study of Constituent, Dispersoid, and Hardening Particles in the Fracture of 7075 Aluminum Alloys, AFML-TR-76-200, Air Force Materials Laboratory Technical Report, (March 1977). \*

\*Available through NTIS, Department of Commerce, 5285 Port Royal Road, Springfield, VA. 22151

## APPENDIX A

### ANALYSIS OF VARIANCE ON NOTCHED FATIGUE DATA

One of the underlying assumptions imposed for valid results for an analysis of variance is that there is equal variance among the test cells, Reference 22. That is to say, the standard deviation between the test cells must be approximately equal.

The variance between test cells in the present study was not constant. The range, the difference between the high and low value of  $N_f$  (i.e.,  $N_f^5 - N_f^1$ ) is an estimator for the variability among the observations. Table A1 gives the observed ranges among four alloys tested under various conditions. Within any load level the variance among the test cells is far from constant. In cases where all the assumptions for an analysis of variance are not precisely met, one can apply an appropriate transformation to the original data if certain criteria are met, Reference 23. In the present case, the data were transformed by taking the common logarithm of  $N_f$ . Since S-N data are plotted on a semi-log scale, this is a logical choice. The range calculated from the transformed data (i.e.,  $\log N_f^5 - \log N_f^1$  not  $\log(N_f^5 - N_f^1)$ ) is given in Table A2. It clearly shows a more constant variability among the eight test cells at each load level and thus more nearly satisfies the assumption of homogeneous variation.

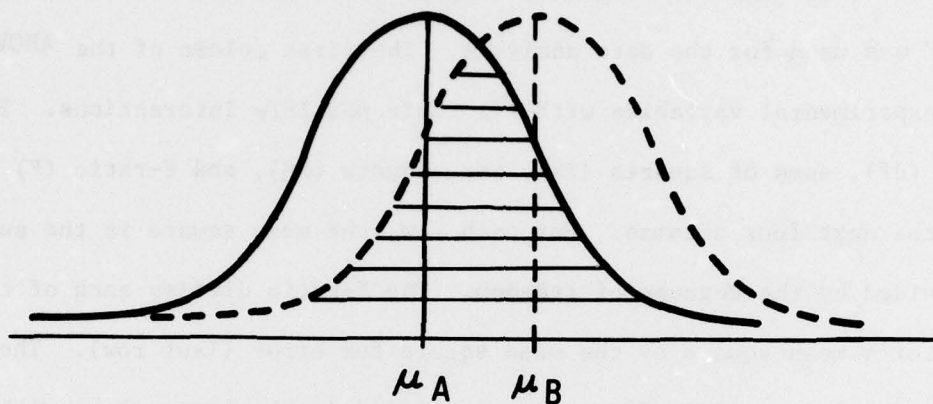
The analysis of variance determines when a statistically significant variation exists between the average number of cycles to failure,  $N_f$ . Figure A1 depicts schematically the contrast between statistically different ( $\mu_C - \mu_D$ ) and not statistically different ( $\mu_A - \mu_B$ ) average values. The experimenter determines how much overlap may exist before calling two averages statistically different. In the present work, this level of significance was set at 1%. This means if the

experiment was repeated many times, and there was no significant difference between test environments, for example, then the correct decision would not be made on average 1% of the time.

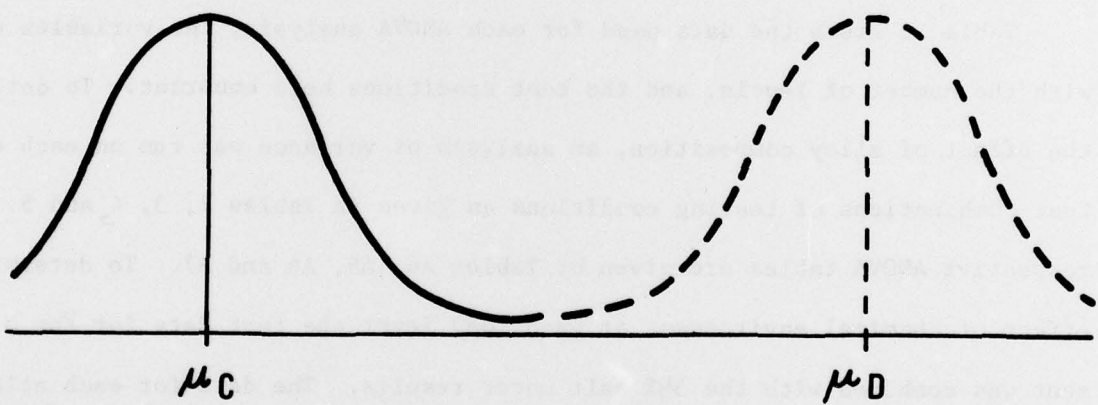
The Biomedical Computer Program: "Analysis of Variance for Factorial Design--2V" was used for the data analysis. The first column of the ANOVA tables gives the experimental variables with all their possible interactions. The degrees of freedom (df), sums of squares (SS), mean square (MS), and F-ratio (F) are listed in the next four columns. For each row, the mean square is the sum of the squares divided by the degrees of freedom. The F-ratio divides each of the experimental factor's mean square by the mean square for error (last row). The critical value (CV) with  $1-\alpha$  equal to 99 percent is listed in the last column with significant interactions noted by an asterisk. Results are rounded off from the computer output, giving only three decimal places.

Table A3 lists the data used for each ANOVA analysis, the variables considered with the number of levels, and the test conditions held constant. To determine the effect of alloy composition, an analysis of variance was run on each of the four combinations of testing conditions as given in Tables 2, 3, 4, and 5. The respective ANOVA tables are given by Tables A4, A5, A6 and A7. To determine the effect of chemical environment at each load level the test data for the oil environment was combined with the 3½% salt water results. The data for each alloy in Table 4 is combined with the respective alloys in Table 2. Similarly, at the higher-load level, Table 5 data is combined with the same alloys in Table 3. Thus, only part of the data from Tables 2 and 3 is combined with Tables 4 and 5 to determine the synergistic effects of alloy composition and chemical environment on the notched fatigue life. The ANOVA tables are given respectively in Tables A-8 and A-9.

## **ANALYSIS OF VARIANCE (ANOVA)**



**(A) NOT STATISTICALLY DIFFERENT DUE TO SMALL SAMPLE SIZE**



**(B) STATISTICALLY DIFFERENT EVEN WITH SMALL SAMPLE SIZE**

**FIGURE A1. SCHEMATIC DIAGRAM ILLUSTRATING THE ANALYSIS OF VARIANCE.**

TABLE A-1. THE NONEQUAL RANGE FOR  $N_f$  BETWEEN THE TWO CHEMICAL ENVIRONMENTS AMONG FOUR EXPERIMENTAL ALLOYS

	ALLOY	B	D	B1	D1
$+12 \text{ ksi}$ $(+82.8 \text{ MPa})$	oil	9129.5	5318.7	5368.0	1881.1
	$3\frac{1}{2}\%$ salt water	693.5	169.8	425.1	353.1
$+18 \text{ ksi}$ $(+124.2 \text{ MPa})$	oil	136.1	193.7	49.1	43.1
	$3\frac{1}{2}\%$ salt water	30.6	12.4	15.5	8.7

TABLE A-2. THE RANGE FOR LOG  $N_f$  BETWEEN THE TWO CHEMICAL ENVIRONMENTS AMONG FOUR EXPERIMENTAL ALLOYS

	ALLOY	B	D	B1	D1
$+12 \text{ ksi}$ $(+82.8 \text{ MPa})$	oil	0.79	0.81	0.74	0.76
	$3\frac{1}{2}\%$ salt water	1.34	0.46	0.67	0.78
$+18 \text{ ksi}$ $(+124.2 \text{ MPa})$	oil	0.55	0.43	0.25	0.25
	$3\frac{1}{2}\%$ salt water	0.61	0.36	0.26	0.22

TABLE A-3. LIST OF ANOVA TABLES

APPENDIX TABLE NOS	DATA FROM TABLE NOS	VARIABLES* (LEVELS)	CONDITIONS HELD CONSTANT	PURPOSE
A-4	2	P(5) D(2)	+12 ksi(82.8 MPa) oil	To determine the effect of alloy composition
A-5	3	P(5) D(2)	+1.8 ksi(124.2MPa) oil	To determine the effect of alloy composition
A-6	4	P(2) D(2)	+12 ksi(82.8 MPa) 3½% salt, water	To determine the effect of alloy composition
A-7	5	P(2) D(2)	+1.8 ksi(124.2MPa) 3½% salt water	To determine the effect of alloy composition
A-8	2+alloy B, Bl, D, D1 data in 4	E(2) P(2) D(2)	+12 ksi(82.8 MPa)	To determine the effect of environment
A-9	3+alloy B, Bl, D, D1 data in 5	E(2) P(2) D(2)	+1.8 ksi(124.2MPa)	To determine the effect of environment

\* P : purity level  
 D : dispersoid type  
 E : environment

TABLE A-4. ANOVA TO DETERMINE THE EFFECT OF ALLOY COMPOSITION FOR SPECIMENS CYCLED AT  $\pm 12$  KSI (82.8 MPa) IN THE OIL ENVIRONMENT.

VARIABLE	df	SS	MS	F RATIO	CV (99%)
D	1	0.611	0.611	5.336	7.34
P	4	2.530	0.633	5.520	*3.85
D'P	4	1.056	0.264	2.303	3.85
error	39†	4.469	0.115	-	-

† One degree of freedom was lost as one replicate test was missing due to a broken cycle counter.

TABLE A5. ANOVA TO DETERMINE THE EFFECT OF ALLOY COMPOSITION  
FOR SPECIMENS CYCLED AT  $\pm 18$  KSI (124.2 MPa) IN THE  
OIL ENVIRONMENT

VARIABLE	df	SS	MS	F RATIO	CV (99%)
D	1	0.249	0.249	3.369	7.31
P	4	0.359	0.090	1.215	3.83
D·P	4	0.684	0.171	2.313	3.83
error	40	2.957	0.074	-	-

TABLE A6. ANOVA TO DETERMINE THE EFFECT OF ALLOY COMPOSITION  
FOR SPECIMENS CYCLED AT  $\pm 12$  KSI (82.8 MPa) IN THE  
 $3\frac{1}{2}\%$  SALT WATER ENVIRONMENT

VARIABLE	df	SS	MS	F RATIO	CV (99%)
D	1	0.024	0.024	0.204	8.53
P	1	0.151	0.151	1.301	8.53
D·P	1	0.076	0.076	0.654	8.53
error	16	1.852	0.116	-	-

TABLE A7. ANOVA TO DETERMINE THE EFFECT OF ALLOY COMPOSITION  
FOR SPECIMENS CYCLED AT  $\pm 18$  KSI (124.2 MPa) IN THE  
 $3\frac{1}{2}\%$  SALT WATER ENVIRONMENT

VARIABLE	df	SS	MS	F RATIO	CV (99%)
D	1	0.001	0.001	0.035	8.53
P	1	0.163	0.163	5.962	8.53
D•P	1	0.009	0.009	0.331	8.53
error	16	0.437	0.027	-	-

TABLE A8. ANOVA TO DETERMINE THE EFFECT OF ENVIRONMENT FOR SPECIMENS CYCLED AT +12 KSI (82.8 MPa)

VARIABLE	df	SS	MS	F RATIO	CV (99%)
E	1	13.985	13.985	135.825	*7.51
D	1	0.163	0.163	1.585	7.51
P	1	0.665	0.665	6.456	7.51
E·D	1	0.386	0.386	3.751	7.51
E·P	1	0.071	0.071	0.689	7.51
D·P	1	0.181	0.181	1.759	7.51
E·D·P	1	0.001	0.001	0.013	7.51
error	32	3.295	0.103	-	-

TABLE A9. ANOVA TO DETERMINE THE EFFECT OF ENVIRONMENT FOR SPECIMENS CYCLED AT +18 KSI (124.2 MPa)

VARIABLE	df	SS	MS	F RATIO	CV (99%)
E	1	5.353	5.353	190.964	*7.51
D	1	0.173	0.173	6.162	7.51
P	1	0.049	0.049	1.757	7.51
E·D	1	0.211	0.211	7.538	*7.51
E·P	1	0.122	0.122	4.346	7.51
D·P	1	0.032	0.032	1.127	7.51
E·D·P	1	0.097	0.097	3.477	7.51
error	32	0.897	0.028	-	-